Journal Homepage: -www.journalijar.com vcvc

INTERNATIONAL JOURNAL OF ADVANCED RESEARCH (IJAR)

ISSN NO. 2320-5407

Article DOI:10.21474/IJAR01/14568
DOI URL: http://dx.doi.org/10.21474/IJAR01/14568

RESEARCH ARTICLE

INVESTIGATION OF THE EFFECT OF ETCHING CURRENT ON TEXTURED SILICON SURFACE FOR FORMING POROUS SILICON LAYERS ACTING AS AN ANTI-REFLECTION COATING.

H.M. Abd-Elrasol[1], M.A. Farag[2], G.M. Youssef[2] and H.A. Elzahed[1]

1. Department of Physics, Faculty of women for Arts, Science and Education, Ain Shams University.
2. Department of Physics, Faculty of Science, Ain Shams University.

……………………………………………………………………………………………………....

Manuscript Info

……………………….

Manuscript History
Received: 20 February 2022
Final Accepted: 24 March 2022
Published: April 2022

Abstract

………………………………………………………………

The porous silicon layers (PSLs) acting as an anti-reflection coating (ARC) formed with different surface porosities are prepared on n+ p textured crystalline CZ- silicon by electrochemical etching (ECE) in HF-based electrolyte using different current densities. The morphological properties of the PSLs are investigated by scanning electron microscopy (SEM). The results show that the porous silicon structure had a smaller pore size range, and the optical properties of the textured surfaces are studied using photoluminescence "PL" and reflectivity measurements. The band gap energy of the prepared PSLs increases to 1.980 eV. The reflectivity of the PSLs decreases to 0.75% in a wavelength range (350–750) nm. The current-voltage (I-V) characteristics of Al/ PS/n^+ p/Al junction are investigated which reveal an increment in the resulting short-circuit current density and the open-circuit voltage up to 5.40 mA/cm^2 and 0.62 V, respectively. These results show an improvement in the fill factor by 57%. The photosensitivity of PSLs solar cells showed a noticeable enhancement in quantum efficiency of the PS cells by increasing the porosity.

……………………………………………………………………………………………………....

Introduction:-

With the increasingly serious energy crisis, solar energy has been given special attention due to its economic, renewable characteristics. The energy wavelength of solar radiation is mainly from visible light to near infrared. Silicon, as an indirect band gap semiconductor material, has a band gap width of 1.12 eV [1], which can have strong intrinsic absorption of photon energy in the wavelength ranges of 300 nm to 1100 nm[2]. Based on this characteristic, it can be applied to solar photovoltaic cells, photoelectric sensors, photo thermal radiationand other fields[3]. However, due to reflection more than 30% of the photon energy on the silicon surface will be lost [4]. This is an important reason thatrestricts solar energy utilization rate of silicon material. Reducing the surface reflectivity of crystal silicon is a way to improve the utilization rate of photonic energy.inserting the surface area of silicon can be extremely enlarged by electrochemical etching and formation of porous layer, Porous silicon seems to be an promising choice due to its fast and easy fabrication by electrochemical etching, large surface area, various accessible pore sizes and morphologies and controllable surface modification [5]. The discovery of porous silicon (PS) by Uhlir in 1956 opened the door for new applications in micro-and optoelectronics, such as chemical sensors, sacrificial/separation layers, light emitting diodes and passive optical filters [6].

Corresponding Author:- H.M.Abd-Elrasol
Address**:-** Department of Physics, Faculty of Girls for Arts, Science and Education, Ain Shams University.

Porous silicon (PS) is a material with a fragile microstructure which allows pores into the internal structure. It is a multilateral material that can be made with specified optical, mechanical, structural, thermal, chemical, and electrical properties. These properties make to be interesting materials to use in different applications [7]. Its high reflectance can be controlled through different techniques such as antireflective coating (ARC), formation of pores and texturizing. Texturizing can enhance surface roughness and has been employed as a common solution for increasing the absorption coefficient [8]. Porous silicon has introduced itself as an attractive material in the optoelectronic devices due to its wide optical transmission range (700–1000 nm), large internal surface area, photoluminescence (PL) properties, and lower effective refractive index[9]. Pyramidal silicon alongside porous silicon is a reasonable structure which can serve as an antireflective layer to resolve the issue of high reflection coefficient in the silicon substrates. In recent years, a variety of methods have been reported for the formation of porosity, among which chemical and electrochemical methods can be mentioned. For instance, the shape of pyramidal structure was changed by stain etching methods for fabricating porous layers[10, 11].

Among these methods, electrochemical etching is a common method for preparing porous silicon because it is efficient and inexpensive[12]. Due to variations in parameters such as electrolyte, current density, etching time and silicon wafer resistivity, different porous silicon (sponge structure and straight pore structure) can be obtained in the electrochemical method for preparing porous silicon[13].

In previous studies, it was found that porous silicon with sponge structure and straight-hole structure had different optical reflection properties[14, 15]. In order to further improve the antireflection performance of porous silicon, the difference in reflectivity between ordered porous silicon structure and disordered multi-structure was studied [1].

The disordered porous structure was found to have lower reflection performance, which was consistent with the structure of porous silicon prepared by electrochemical etching[3].

Currently, many experimental studies focus on studying the optical and the electrical properties of Si-based porous materials, from Nano- to macro-scale, by changing the anodization conditions and hence changing the porosity. The change in pore diameters (pores walls dimensions) has become very important for numerous applications such as photonics, optoelectronics, electronics, biosensors, chemical sensors, and solar cells [16]. In solar cell applications, it is desired to create an appropriate roughness on the device front surface to trap sunlight as much as possible [17-20].

The main objective of this work is to investigate the effect of PS surface texturing (roughness) on the optical properties of solar cells. The reflectivity and PL have been investigated to show the effect of the etching process on the photons trapping enhancement. The electrical properties of solar cells are also investigated.

Experimental: -

The silicon samples used in this study were using [100] oriented P-type CZ wafers with resistivity ranging from 2 up to 5 Ω.cm with a thickness of 450 μm [21]. Before electrochemical etching of silicon, silicon substrates were rinsed in de-ionized water and dried in the presence of nitrogen gas after heating in trichloroethylene (isopropyl) for 5 minutes [21].

The PSLs sample was prepared done in the etching solution containing of 48% hydrofluoric acid, 99.9% ethanol, and water with concentration (HF: C_2H_5OH: H_2O = 1:1:1 by volume) at different current densities 5, 10, 15, 20 and 25 mA/cm^2 for time etching 5 min denoted as S1, S2, S3, S4 and S5, respectively. The PSLs have been formed on the n^+ region during electrochemical etching process. The process of PS formation has been carried out in the electrochemical etching cell, which included a platinum electrode as cathode and silicon wafer as anode. After etching, the samples were rinsed in acetone and ethanol and then, dried under nitrogen gas flow. We have investigated the optical properties using the UV–Vis spectrophotometer [Carry 4000 Agilent] provided with integrating sphere for measuring the diffused transmittance and reflectance of the samples, and using Photoluminescence [Spectrofuorometer FP-6500 Jasco] equipped with xenon arc lamp (150 W) as light source, the excitation was obtained using a light wavelength of 325 nm. The structure characterization of the surface was indicated using SEM [Quanta 250 FEG] for samples after and before etching with a magnification power of 1500 X. The current–voltage (I–V) measurements have been investigated by using Keithley 2400 source meter at room temperature under illumination by 200 W an ordinary tungsten filament lamp.

Results and Discussion: -

Morphological characteristics:

Fig. 1 shows the SEM images of the front surface of the cells before and after PS formation. Fig. 1(a) represents the morphology of the un etched surface of the reference cell which shows that it contains a different sizes of spaced pyramids distributed on the whole surface. On the other hand, Fig. 1(b–f) shows the SEM images of the PSLs formed on the samples fabricated with 5,10, 15, 20 and 25 mA/cm^2 current densities. The morphology of different samples shows significant effect of etching current density on the size and shape of the porous pyramids. At etching current density 5 mA/cm^2, no physical pores appeared. By increasing the etching current density to 10 mA/cm^2 Fig. 1(c), the distributed pores became more significant. Moreover, in this sample, the shape of the micro-pyramids remained unchanged, and the pores were identical in different faces of the pyramids. As the etching current increases, it can be seen that the shape of the micro-pyramids was changed. Fig. 1(e), shows that prolonged etching current density (20 mA/cm^2) led to dissolution of pyramidal structures. With increasing the current density, the rate of the formation of oxide islands on silicon surface will be raised, therefore chemical polishing may occur which will lead to damaging the pyramidal structure[22]. The gravitational method [23] has been used to evaluate the percentages of porosity for S1, S2,S3,S4 and S5 samples, which are estimated as 79%, 82%,86%, 84% and 83%, respectively.

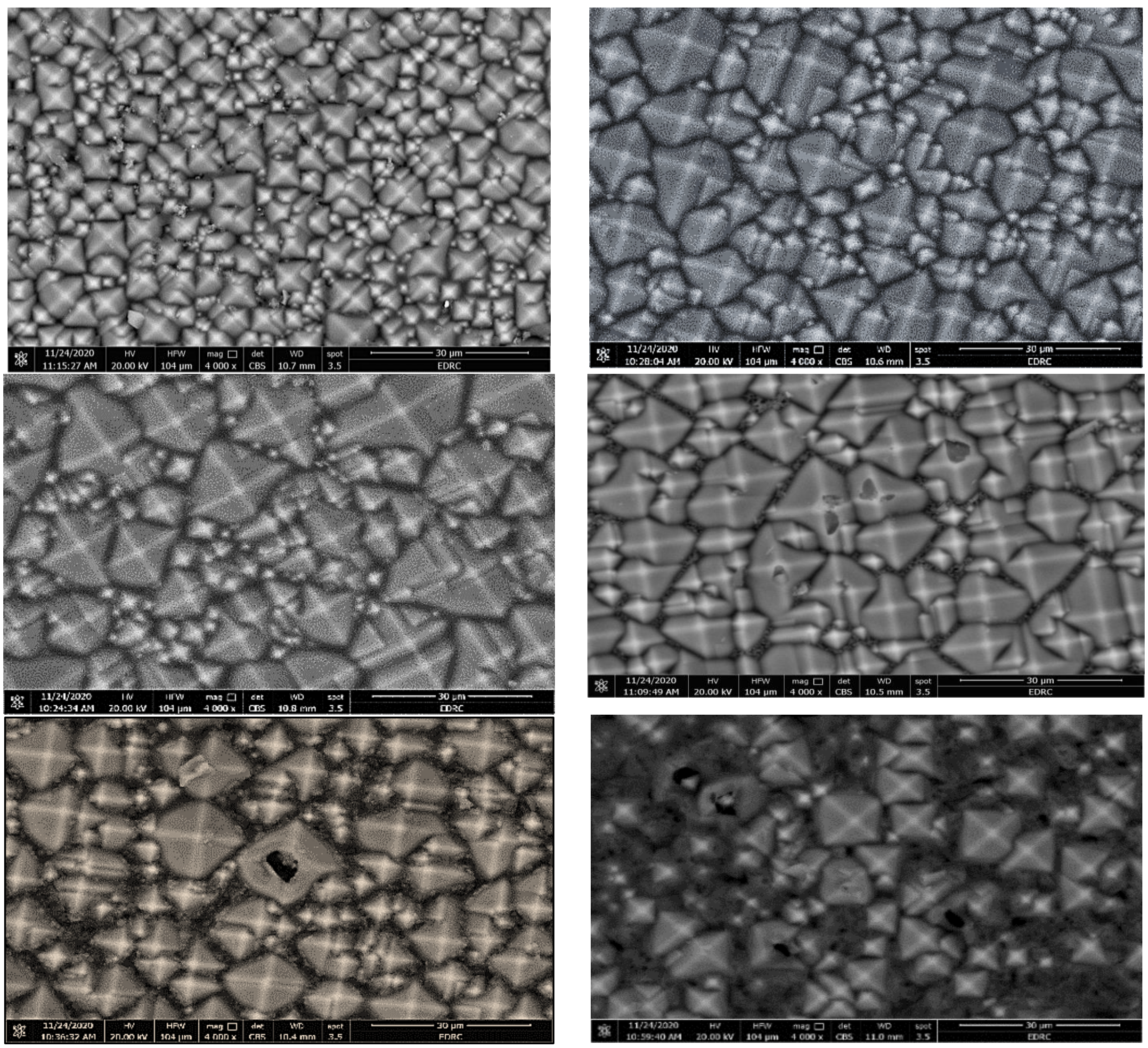

Fig. 1:- SEM images of top view of (a) n+ p solar cell without PS formation (reference) and after PS formation fabricated at (b)5 mA/cm^2 (S1), (c)10 mA/cm^2 (S2), (d) 15mA/cm^2 (S3), (e) 20mA/ cm^2 (S4) and (f) 25mA/cm$_2$ (S5).

Photoluminescence of PS layers and determination of pore size:

Fig. 2 shows the photoluminescence (PL) spectra of the porous-pyramidal samples etched at different current densities at room temperature. The fig shows that the created porous layers result in an emission band over the visible light region. The highest PL intensity was observed for the porous pyramidal sample S5 owing to its high surface area resulting in an increment in the incident light absorption and hence higher generation of electron-hole The energy gap of all the PS layers is calculated by by using Plank's- Einstein equation

$$E_g = \frac{hc}{\lambda} \qquad (1)$$

where h is the Planck's constant, c is the speed of light and λ_{max} is the wavelength corresponding to the peak of PL spectra. The resultant values of (d) for all the PS samples are summarized in Table 1.

As can be seen from Table 1, the optical energy bandgap is higher for PS layers prepared with higher etching time. The obtained E_g values of PS are higher than the corresponding value for silicon single crystal (1.12 eV) [24]which is attributed to the creation of porous layer with small pore size [25].. In addition, this means that the particles are confined into lower dimension and the probability of the recombination of the electrons and holes is higher in low dimensional structures according to quantum confinement effects[26]. The energy band gap of PS samples is directly proportional to the increase of etching current confirming the blue shift in the PL peak.

The observed increase in PL intensity could be attributed to the increment of the pores volume by etching[20, 27]. Using the calculated E_g values from PL spectra, the pore diameter, d, is calculated using the following equation [9]:

$$E(eV) = E_g + \frac{h^2}{8d^2}\left[\frac{1}{m_e^*} + \frac{1}{m_h^*}\right] \qquad (2)$$

where E (eV) is the energy band gap of PS calculated from the PL peak position of the PS layer as shown in Fig. 2, E_g= 1.12 eV is the energy band gap of bulk Si, h is Planck's constant = 4.13 x 10^{-15} eV s andm_e^*, $m_h^*$are the electron and hole effective mass, respectively (at 300 K, m_e^*= 0.19 m_o,m_h^* =0.16m_o where m_o=9.109 x10^{-31} Kg) .The resultant values of (d) for all the PS samples are calculated and summarized in Table 1

Table 1:- The optical energy bandgap and pore size of PS and the calculated refractive indices using Ravindra Et Al [a]Herve and Vandamme [b] and Ghosh Et Al[c] Models.

Etching current density (mA/cm²)	Eg (eV)	D(nm)	Eg calculated from "R" (eV)	refractive index "n"
5 (S1)	1.899	5.230	1.821	2.77[a] 2.91[b] 2.79[c]
10 (S2)	1.901	5.220	1.958	2.72[a] 2.83[b] 2.72[c]
15 (S3)	1.905	5.210	1.980	2.71[a] 2.82[b] 2.71[c]
20 (S4)	1.898	5.234	1.913	2.74[a] 2.86[b] 2.74[c]
25(S5)	1.899	5.230	1.883	2.75[a] 2.88[b] 2.76[c]

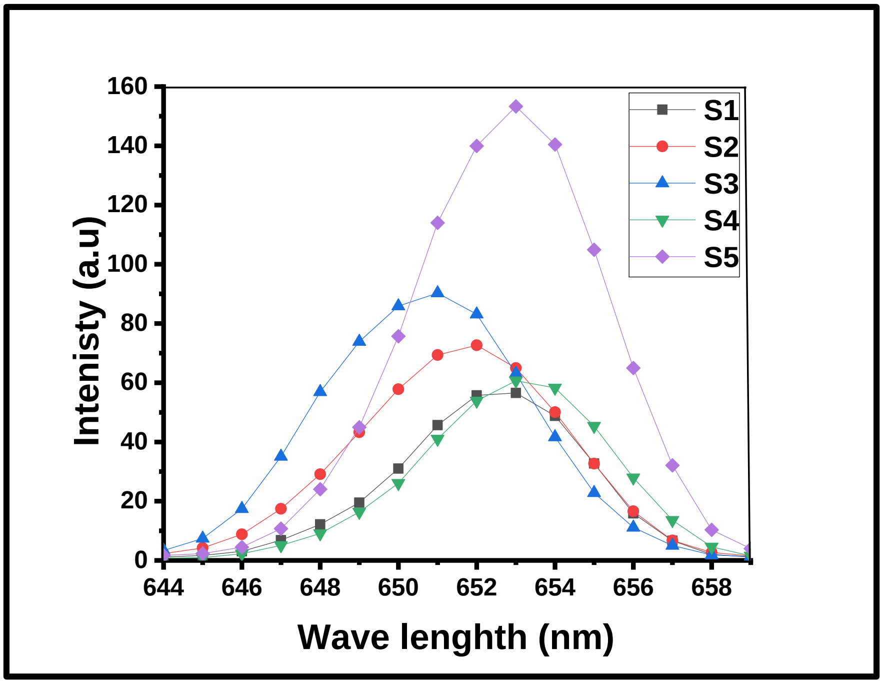

Fig. 2:- Photoluminescence spectrum of PSLs samples.

The effective refractive index of porous silicon has been shown to be dependent on the degree of porosity attained [28]. Different attempts have been investigated to relate the refractive index and the energy gap Eg through simple empirical relationships [16].

Moss [29]presented the following equation, based on an atomic model:

$n^4Eg= K$ (3)

where the constant K is and was found to be 108 eV by Ravindra et al. Later on Ravindra et al.[30] suggested a linear relationship between the band gap Eg and the high frequency refractive index;

$n=\alpha+\beta Eg$ (4)

where $\alpha=4.048$, $\beta=-0.62V^{-1}$

Herve and Vandamme [31]also proposed an empirical relation;

$n=\sqrt{1+(\frac{A}{Eg+B})}$ (5)

where A=13.6eV, B=3.4eV

Ghosh et al.[32] took a different approach to the problem by considering the band structural and quantum dielectric formulations of Penn (PENN 1975) and Van Vechten (Vechten 1969). The expression for the high-frequency refractive index can be written as;

$(n)^2-1=(\frac{A}{Eg+B})^2$ (6)

where A=25Eg+212, B=0.21Eg+4.25

The calculated refractive indices using the three approaches are presented in Table1.

3.3. UV–Vis spectrophotometry: -

The change of the PS surface texturing during the etching process makes the PSL as a good ARC layer in manufacturing solar cells. Since, the surface textured reduces the light reflection and increases the light trapping upon wide wavelength range[16]. In previous studies, the best reflectivity of porous silicon is about 4.7% under the incident light wave of 300– 1000 nm [33]. so, it is still important to improve the light energy utilization efficiency by reducing the reflection efficiency of silicon antireflection layer. In order to estimate the optical antireflective ability of porous silicon samples, the total reflectivity of the samples has been measured by an ultraviolet–visible spectrophotometer under normal incidence condition.

Fig.3 shows the diffused reflectance spectra for the PS textured samples with different porosity in comparison with the reference sample. The figure showed that the PS samples provide lower reflectivity than the un etched C-Si such that The average reflectance of the un etched c-Si is ~ 18 %, but the average reflectance of the porous pyramidal structures at different etching current (S1, S2, S3, S4, S5) in the same spectral range are ≅7 %, 3.7 %, 2 %, 2.7 % and, 4 %, respectively.

The minimum reflectance which was obtained for the porous pyramidal structure formed at $15mA/cm^2$ is due to its higher surface area and enhanced light capturing ability of this sample. The results showed that the combination of pyramids and optimized porous structures can improve the optical absorption of silicon substrates by increasing the specific surface area. Thus, this combination can be used as an antireflective layer in high-efficiency optoelectronic devices such as photodetectors.

In addition to, these results demonstrate that PS has the ability for increasing light absorption in the VIS region of the solar spectrum, which plays an important role for improvement of the solar cell efficiency[34].

Another way to obtain the energy band gap value is to calculate the absorption coefficient using the reflectance spectrograph as mention in the following Eq. [35]

$$\alpha = \frac{1}{2t}\ln\frac{(R_{max}-R_{min})}{(R-R_{min})} \quad (3)$$

where α is the Absorption coefficient, t is the thickness of the film, R_{max}, R_{min} are the maximum and minimum reflectance in the diffused refection spectra and R is the reflectance for any intermediate energy photons recorded by the spectrophotometer, the Eg can be calculated using the following Eq [36].

$$\alpha h\nu = A(h\nu - E_g)^m \quad (4)$$

where (A) is the edge width parameter and (Eg) is the optical energy gap of the material. The parameter (m) represents the type of transition; For indirect transition (m=2) and direct transition (m=1/2). By plotting a graph of $(\alpha h\nu)^{1/2}$ versus (hν), the intercept of extrapolation to zero absorption with the photon energy axis is the Eg value. The graphs of the silicon and PS with different etching current are shown in Fig. 3.

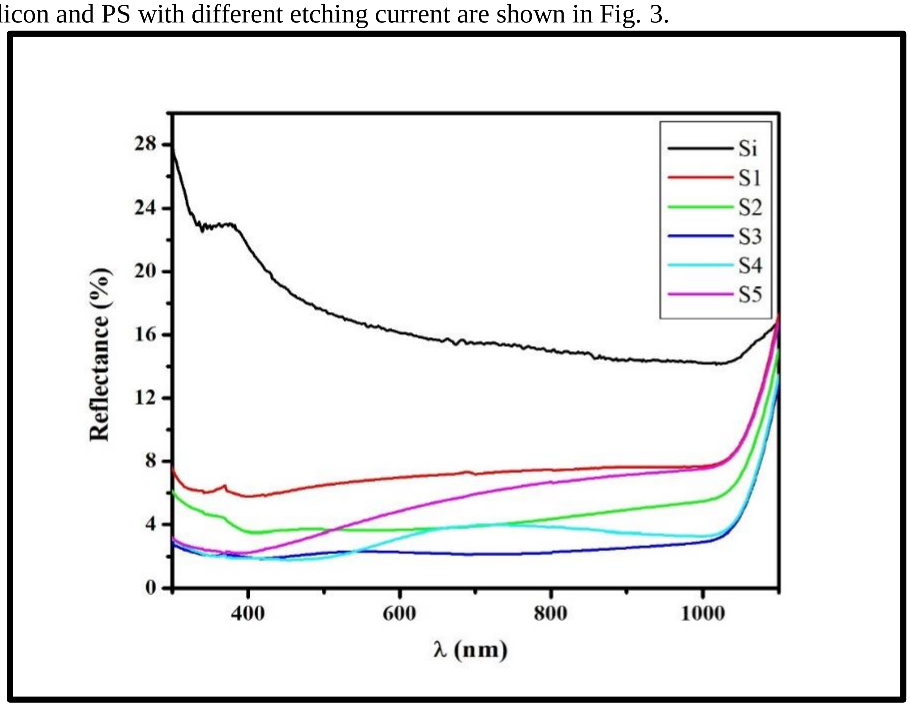

Fig. 3:-The reflectivity spectra of the PSLs compared to the un etched C-Si sample.

Fig. (4) shows the plot of $(\alpha h\nu)^{1/2}$ versus hυ, which is used to calculate the energy band gap, considering an indirect allowed transition of PS samples compared with the C-Si sample. It is easy to observe that the indirect energy band gap increases from 1.8213 to 1.980 ev with the increment of the etching current density. These results also confirm that PS, has an indirect band gap [37]. The values of the energy bandgap were calculated in Table 1 and the results are matched so far with the previous values of the PL method.

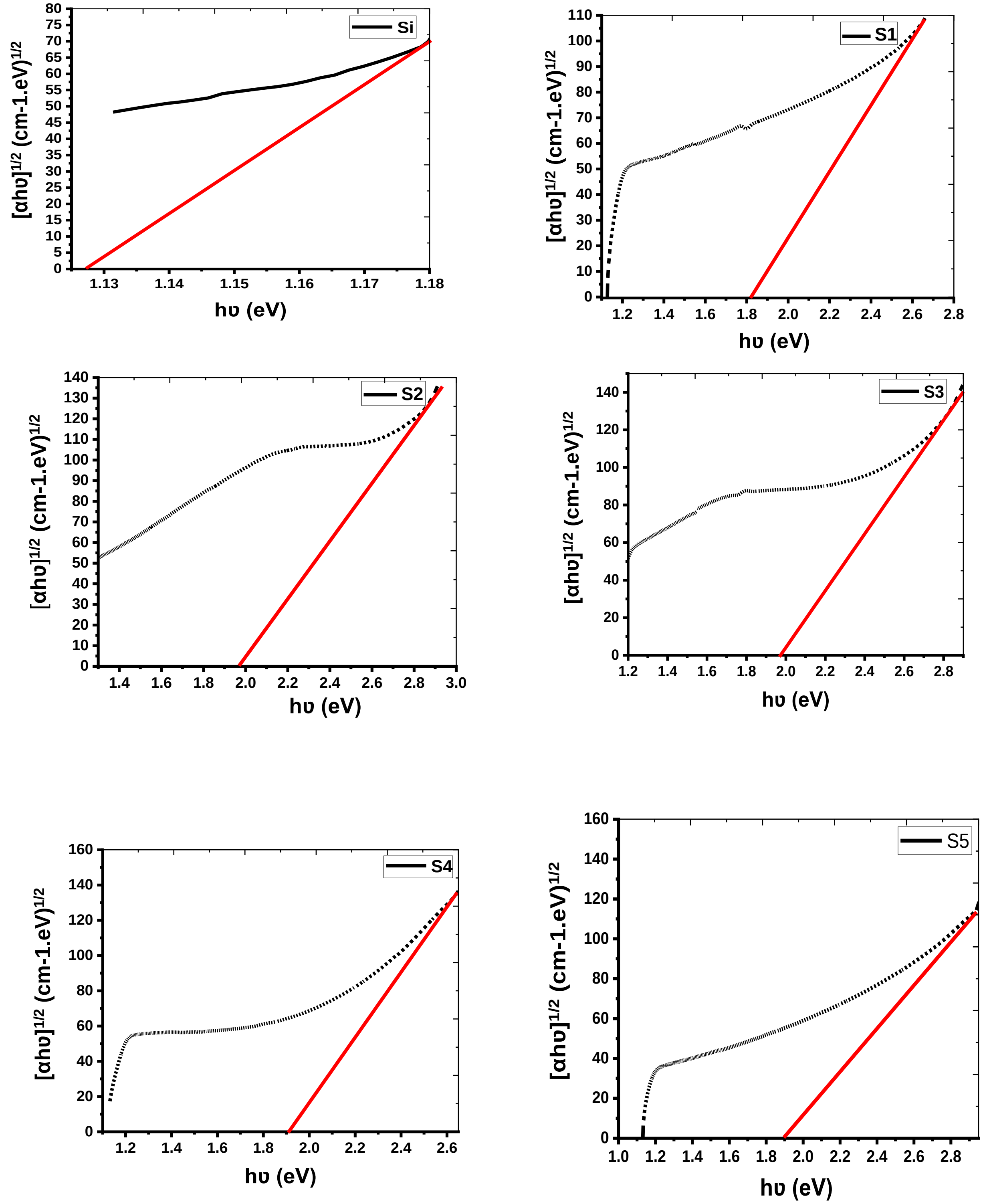

Fig. (4):- $(\alpha h\upsilon)^{1/2}$ versus hυ for indirect allowed transitions in the C-Si compared with the PS samples

J–V characteristics under illumination:-

The increase in the absorption is in prospect to improve solar cells efficiency. Under a constant illumination condition for power density (100 mW/cm²), the current density–voltage (J–V) characteristics are measured for the reference n^+p Si solar cell and corresponding solar cells fabricated with PS layers as shown in Fig 5

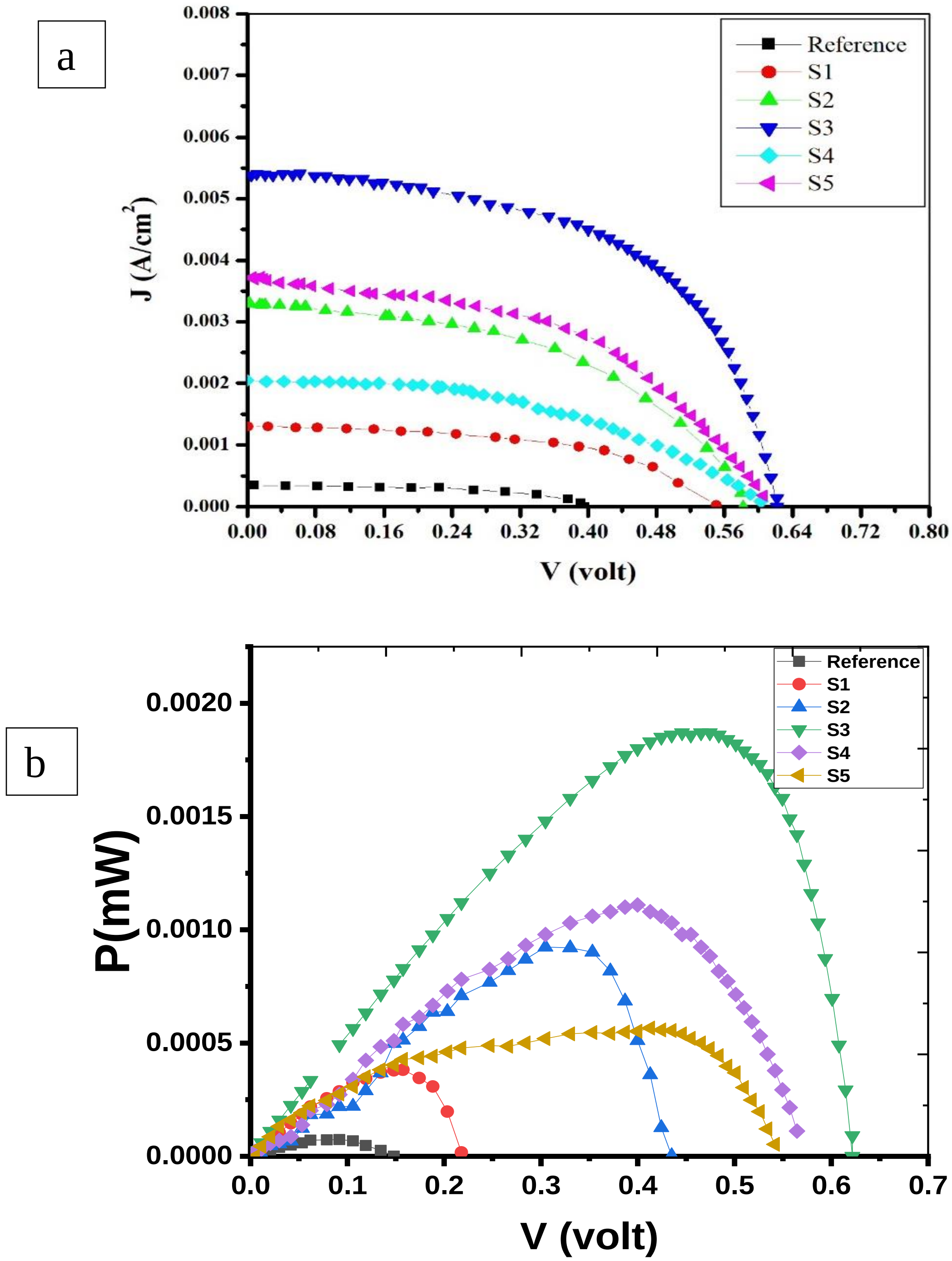

Fig. 5:- (a) Current density-voltage (J-V) characteristics ofthe PSLs under illumination. (b) The relation between the power and the voltage

The relation shows a good enhancement of the photovoltaic performances of cells S1, S2 and S3 as compared to the untreated one and then decreased for the cells S4 and S5.

From this figure, the short-circuit current density (J_{SC}), open-circuit voltage (V_{OC}) of the cells were obtained and are listed in Table 2.

Table 2:- The calculated values of the Jsc, Voc, and FF.

Sample	**V_{OC} (volt)**	**J_{SC} (A/cm^2)**	**FF**
Reference	0.39	0.0004	0.50
S1	0.55	0.0013	0.54
S2	0.58	0.0033	0.56
S3	0.62	0.0054	0.57
S4	0.62	0.0037	0.49
S5	0.61	0.0021	0.47

The obtained results shown that the short-circuit current density(JSC) increased from 10 to 15 mA/cm^2 and **V_{oc}** increased from 390 and 620 mV for the cells S1 and S3, respectively when compared to the solar cell without a PS layer.

The enhancement of J_{SC} and V_{OC} could be due to the photo generation in PS and the formation of a heterojunction between porous layer and Si substrate (reference sample). In addition to, the enhancement could be also due the enhancement in the optical path length and light capturing [38]] which leads to increasing the photo generated carriers and thus significantly improve the solar cell parameters [39].

The fill factor (FF) which is defined as the ratio between the maximum power and the product of the short-circuit current with the open-circuit voltage is given by [40]:

$$FF = \frac{J_{max}\ V_{max}}{J_{sc}\ V_{oc}} \qquad (5)$$

Where Im is the maximum current, Vm is the maximum voltage, and FF is a fill factor. The values of FF are also calculated and listed in Table 2. The results show an enhancement in FF values for the solar cells with PS layers. The value of FF increases from 0.54 to 0.57 with increasing etching current density to 15 mA/cm^2 due to increasing the values of the Voc, Jsc and then decreased to 0.49, 0.47 for the cells S4 and S5 respectively.

Finally, the improvement in the V_{oc}, J_{sc} and FF values of the solar cells with PS layer could enhance the electrical properties and increase the conversion efficiency of Si solar cells [41]. The results published in the earlier article [42] agree with our results.

Conclusion:-

We verified a simple technique for fabricating porous silicon (PS) layers on the front part of n^+ p Si junctions. This technique was formed by electrochemical etching with different current densities (5, 10, 15, 20 and 25 mA/cm^2) and the etching time was 5 min. The SEM shows that the porosity on the front side of Si increases with the increase of etching current density. The results show a strong antireflection of porous-pyramids structured silicon surface which was obtained by increasing the etching current compared to the untreated textured silicon surface. Electrical conduction of Al/PS/n^+ p/Al junction fabricated at different current densities was determined and compared with the un etched reference sample. Under illumination, the short-circuit current density, the open-circuit voltage and fill factor are enhanced by increasing porosity which show that the low-cost formation of PSL can act as good passivation layer for uses in solar cells.

In addition, the photoelectrical conversion of the porous silicon solar cells increases with increasing etching up to the etching current density of 15 mA/cm2, and then started to decrease which is correlated to the variation of the photovoltaic parameters. Finally, the optimum condition of the porous silicon cells prepared with a concentration of HF: C_2H_5OH: H_2O = 1:1:1 by volume for 5 min gives higher photoelectrical conversion efficiency is at a current density 15 mA/cm^2.

References:-

1. Ge, D., et al., Optimization of porous silicon structure as antireflective material. The European Physical Journal D, 2022. 76(2): p. 1-8.

2. Philipp, H. and E. Taft, Optical constants of silicon in the region 1 to 10 eV. Physical Review, 1960. 120(1): p. 37.
3. Srivastava, A., et al., Highly efficient PEDOT: PSS/silicon hybrid solar cells via effective surface microengineering of low-cost solar-grade silicon wafers. ACS Applied Energy Materials, 2021. 4(4): p. 4181-4198.
4. Caño, P., et al., GaAsP/SiGe tandem solar cells on porous Si substrates. Solar Energy, 2021. 230: p. 925-934.
5. G.M.Youssef ,ayahame,et al The behaviour of IV characteristics of porous silicon upon different sugars of various, International Journal of Advanced Research in Science,Engineering and Technology concentrations 2021
6. G.M.Youssef., et al. "Investigation of size and band gap distributions of Si nanoparticles from morphology and optical properties of porous silicon layers formed on a textured N+ P silicon solar cell." Int. J. Semicond. Sci. Technol 6 (2016): 1-12.
7. Abood, M.K., et al., Effect of ZnO nanoparticles deposition on porous silicon solar cell. Materials Today: Proceedings, 2021. 42: p. 2935-2940.
8. Fallahazad, P., et al., Porous pyramidal silicon structures for improved light sensing performance. Optik, 2020. 222: p. 165433.
9. Salman, K.A., Z. Hassan, and K. Omar, Effect of silicon porosity on solar cell efficiency. Int. J. Electrochem. Sci, 2012. 7(9): p. 376-386.
10. Naderi, N. and M. Hashim, Nanocrystalline SiC sputtered on porous silicon substrate after annealing. Materials Letters, 2013. 97: p. 90-92.
11. Azeredo, B.P., et al., Direct imprinting of porous silicon via metal-assisted chemical etching. Advanced Functional Materials, 2016. 26(17): p. 2929-2939.
12. Du, Q.G., et al., Enhanced optical absorption in nanopatterned silicon thin films with a nano-cone-hole structure for photovoltaic applications. Optics letters, 2011. 36(9): p. 1713-1715.
13. Mohamed, B.R., H. Anouar, and B. Brahim, Improvement of multicrystalline silicon solar cell performance via chemical vapor etching method-based porous silicon nanostructures. Solar Energy, 2012. 86(5): p. 1411-1415.
14. Carstensen, J., M. Christophersen, and H. Föll, Pore formation mechanisms for the Si-HF system. Materials Science and Engineering: B, 2000. 69: p. 23-28.
15. Bisi, O., S. Ossicini, and L. Pavesi, Porous silicon: a quantum sponge structure for silicon based optoelectronics. Surface science reports, 2000. 38(1-3): p. 1-126.
16. G.M.Youssef ,Ahmed, et al., Investigation of Porous Silicon Layers Properties Using Speckle Techniques for Photovoltaic Applications. Silicon, 2020. 12(7): p. 1603-1617.
17. Maniya, N.H., J. Ashokan, and D.N. Srivastava. Application of porous silicon in solar cell. in AIP Conference Proceedings. 2018. AIP Publishing LLC.
18. Praveenkumar, S., et al., An experimental study of optoelectronic properties of porous silicon for solar cell application. Optik, 2019. 178: p. 216-223.
19. Li, M., et al., Metal-assisted chemical etching for designable monocrystalline silicon nanostructure. Materials Research Bulletin, 2016. 76: p. 436-449.
20. Vickers, N.J., Animal communication: when i'm calling you, will you answer too? Current biology, 2017. 27(14): p. R713-R715.
21. G.M.Youssef , H.A. NAWAR, et al. PREPARATION AND PHYSICAL CHARACTERIZAYION OF POROUS SILICON LAYERS FOR SENSING APPLICATIONS,2015
22. Yaakob, S., et al., The formation and morphology of highly doped N-type porous silicon: effect of short etching time at high current density and evidence of simultaneous chemical and electrochemical dissolutions. J. Phys. Sci, 2012. 23(2): p. 17-31.
23. Lee, H., E. Lee, and S. Lee. Investigation of nano-porous silicon antireflection coatings for crystalline silicon solar cells. in 2006 IEEE Nanotechnology Materials and Devices Conference. 2006. IEEE.
24. G.M.Youssef., et al., Investigation of size and band gap distributions of Si nanoparticles from morphology and optical properties of porous silicon layers formed on a textured N+ P silicon solar cell. Int. J. Semicond. Sci. Technol, 2016. 6: p. 1-12.
25. Butturi, M., et al., Effects of ageing on porous silicon photoluminescence: Correlation with FTIR and UV-Vis spectra. Solid state communications, 1997. 101(1): p. 11-16.
26. Nirmal, M. and L. Brus, Luminescence photophysics in semiconductor nanocrystals. Accounts of chemical research, 1999. 32(5): p. 407-414.
27. Losic, D. and A. Santos, Electrochemically engineered nanoporous materials. Methods, Properties and Applications., 2015. 220.

28. Loni, A., et al., Porous silicon multilayer optical waveguides. Thin solid films, 1996. 276(1-2): p. 143-146.
29. Moss, T., A relationship between the refractive index and the infra-red threshold of sensitivity for photoconductors. Proceedings of the Physical Society. Section B, 1950. 63(3): p. 167.
30. Ravindra, N., S. Auluck, and V. Srivastava, On the Penn gap in semiconductors. Physica status solidi (b), 1979. 93(2): p. K155-K160.
31. Herve, P. and L. Vandamme, Empirical temperature dependence of the refractive index of semiconductors. Journal of Applied Physics, 1995. 77(10): p. 5476-5477.
32. Ghosh, D., L. Samanta, and G. Bhar, A simple model for evaluation of refractive indices of some binary and ternary mixed crystals. Infrared Physics, 1984. 24(1): p. 43-47.
33. Kwon, J.-H., S.-H. Lee, and B.-K. Ju, Screen-printed multicrystalline silicon solar cells with porous silicon antireflective layer formed by electrochemical etching. Journal of applied physics, 2007. 101(10): p. 104515.
34. Dzhafarov, T. and A. Bayramov, Porous silicon and solar cells. Handbook of Porous Silicon: Second Edition, 2018. 2(2): p. 1479-1492.
35. Tauc, J. and A. Menth, States in the gap. Journal of non-crystalline solids, 1972. 8: p. 569-585.
36. Canham, L., Handbook of porous silicon. 2014: Springer International Publishing Berlin, Germany:.
37. Bessais, B., et al., Correlation of photoluminescence spectra and structure of porous silicon. Semiconductor science and technology, 1996. 11(12): p. 1815.
38. Zhang, S., et al., Investigation of nanoscale quasi pyramid texture for HIT solar cells using n-type high performance multicrystalline silicon. Energy Procedia, 2017. 124: p. 321-330.
39. Dimova-Malinovska, D., Application of stain etched porous silicon in c-Si solar cells. Opto-Electronics Review, 2000. 8(4): p. 353-355.
40. El-Nahass, M.M., et al., Electrical and photovoltaic properties of FeTPPCl/p-Si heterojunction. Synthetic metals, 2011. 161(21-22): p. 2253-2258.
41. Panek, P., M. Lipiński, and J. Dutkiewicz, Texturization of multicrystalline silicon by wet chemical etching for silicon solar cells. Journal of materials science, 2005. 40(6): p. 1459-1463.
42. Harb, N.H. and F.A.-H. Mutlak, Effect of etching current density on spectroscopic, structural and electrical properties of porous silicon photodetector. Optik, 2022. 249: p. 168298.